NOO TR-232

INTERMEDIATE AND DEEP CURRENT MEASUREMENTS IN THE NORTHEAST PACIFIC OCEAN

Marshall D. Earle

Naval Oceanographic Office

July 1975

Technical Report

Prepared for
Long Range Acoustic Propagation Project
of the Office of Naval Research
and the Chesapeake Division of the
Naval Facilities Engineering Command

Department of the Navy
Naval Oceanographic Office
Washington, D.C. 20373

FOREWORD

The increasing sophistication of Naval weapons systems, both fixed and mobile, requires that oceanographers understand the motions, and the associated driving and physical forces, of oceanic currents. The studies which are prerequisite to such knowledge require a tremendous investment in capital and human resources, but only through such investments will the Navy approach solutions to its environmental problems. This report describes the characteristics of intermediate and deep currents in the central northeast Pacific Ocean, a region where very few direct current observations have been made.

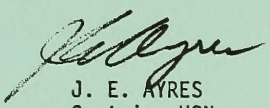

J. E. AYRES
Captain, USN
Commander

UNCLASSIFIED

SECURITY CLASSIFICATION OF THIS PAGE *(When Data Entered)*

REPORT DOCUMENTATION PAGE		READ INSTRUCTIONS BEFORE COMPLETING FORM
1. REPORT NUMBER TR-232	2. GOVT ACCESSION NO.	3. RECIPIENT'S CATALOG NUMBER
4. TITLE *(and Subtitle)* Intermediate and Deep current Measurements in the Northeast Pacific Ocean		5. TYPE OF REPORT & PERIOD COVERED Final 6. PERFORMING ORG. REPORT NUMBER
7. AUTHOR(s) Marshall D. Earle		8. CONTRACT OR GRANT NUMBER(s)
9. PERFORMING ORGANIZATION NAME AND ADDRESS Naval Oceanographic Office Washington, D. C. 20373		10. PROGRAM ELEMENT, PROJECT, TASK AREA & WORK UNIT NUMBERS PE 63795N Proj. No. R2408 Task area R2409 Work Unit 773-LK-REN
11. CONTROLLING OFFICE NAME AND ADDRESS		12. REPORT DATE 13. NUMBER OF PAGES 31
14. MONITORING AGENCY NAME & ADDRESS*(if different from Controlling Office)*		15. SECURITY CLASS. *(of this report)* Unclassified 15a. DECLASSIFICATION/DOWNGRADING SCHEDULE

16. DISTRIBUTION STATEMENT *(of this Report)*

Approved for public release; distribution unlimited

17. DISTRIBUTION STATEMENT *(of the abstract entered in Block 20, if different from Report)*

18. SUPPLEMENTARY NOTES

19. KEY WORDS *(Continue on reverse side if necessary and identify by block number)*

Pacific Ocean, ocean currents, internal tides

20. ABSTRACT *(Continue on reverse side if necessary and identify by block number)*

Ocean currents were measured in the central northeast Pacific, from 30°N to 40°N and 140°W to 150°W, with nine arrays of moored current meters during autumn 1973. Current meter records at depths from 700 m to 5420 m were analyzed to determine the characteristics of intermediate and deep currents within the central northeast Pacific. The currents in this region have very low speeds which generally decrease with increasing depth. Contributions to the time-dependent currents are primarily from oscillatory (over)

DD FORM 1 JAN 73 1473 EDITION OF 1 NOV 65 IS OBSOLETE
S/N 0102-014-6601

UNCLASSIFIED

SECURITY CLASSIFICATION OF THIS PAGE *(When Data Entered)*

motions at the local inertial frequencies and the semidiurnal tidal frequency. Spectral analysis indicates that tidal frequency motion is essentially due to baroclinic internal tides and not barotropic surface tides.

ACKNOWLEDGMENTS

The author thanks the following Naval Oceanographic Office personnel for their assistance: Donald Burns who provided extensive help and many suggestions throughout this study; Louis Banchero, Michael Holland, and Warren Sanborn who placed and successfully recovered the current meter arrays under very difficult working conditions; and Robert Guthrie who provided the time series vector plots and the current speed probability distributions.

CONTENTS

FIGURES

TABLES

INTRODUCTION

Studies of currents in the northeast Pacific, distant from the North American continent, have been mainly based on interpretation or analysis of observed physical and chemical seawater properties. While these classical techniques provide estimates of the mean and very-low-frequency circulation, direct current measurements are required to determine higher frequency time-dependent motion. Very few direct measurements have been reported in the literature. Reid (1962) and Hendershott (1973) found significant diurnal clockwise rotation in several series of GEK (geomagnetic electrokinetograph) measurements of surface currents near 30°N,125°W. Bathythermograph observations in the surface layer did not show significant diurnal vertical isotherm displacements but did show some indications of semidiurnal internal waves. Using neutrally buoyant Swallow floats near 28°N,139°W and 29°N,118°W, Knauss (1962) observed diurnal clockwise rotating currents at depths between 700 m and 3,900 m. Diurnal currents at different depths were not in phase. Bathythermograph (BT) observations by Knauss did not indicate significant vertical displacement of isotherms. Diurnal motions reported by Knauss (1962), Reid (1962), and Hendershott (1973) represent inertial period motion. Current measurements from two moored arrays near 28°N,158°W have been reported (Patzert, Wyrtki, and Santamore, 1970), but the time series of these measurements are too short for statistical analysis.

The objective of this experiment was the direct measurement of intermediate and deep currents over a large area over periods of at least one month. The experiment was not designed as a small-scale study of internal wave characteristics. Guthrie, Burns and Smith (1974) have described some of the data on which this report is based. The results reported herein may later be used as inputs to the design of current measurement programs concentrating on smaller vertical and horizontal scales. These results also will be useful in formulating numerical models to compute intermediate and deep currents in the North Pacific.

DESCRIPTION OF CURRENT METER ARRAYS

Currents were measured in deep water far from the Continental Shelf near the center of the eastern gyre of the North Pacific Ocean (fig. 1). Table 1 provides a description of each of the nine arrays. Most arrays were located over nearly level topography, and no arrays were placed close to seamounts. In order to reduce motion effects due to surface gravity waves, each array was supported by a subsurface buoy at a depth of approximately 500 m. A short section of chain attached to the buoy and 500 m of wire rope supported the first current meter. The remainder of each array consisted of nylon line with current meters suspended at selected depths. Geodyne model 101 current meters were used on arrays A through C, and Geodyne model 102 meters were used on arrays D through I. The recording interval for all meters was 10 minutes. Each array terminated with an acoustic release, steel dampening disk, and concrete anchor clump.

Current meter depths in table 1 are based on the assumption that the nylon line stretched 15 percent of cut length for new line and 12 percent

for used line. To estimate effects of mooring motion, a finite element model (Chhabra, 1973; Chhabra, Dahlen and Froidevaux, 1974) was used to simulate array motion. The highest measured current speed profiles were inputs to the finite element model. Time-dependent displacements of the current meters were found to have a negligible effect on velocity measurements.

DESCRIPTION OF MEASURED CURRENTS

Prior to detailed analysis, all 10-minute current speed and direction values were resolved into east-west and north-south components. To obtain an initial description of the current velocity field, individual components were averaged vectorially to provide half-hour mean current vectors which were plotted as a function of time. Figure 2 is an example of such a plot. The plots indicate that the current speeds are very low and that the most significant contributions to the time-dependent flow are clockwise motions at the semidiurnal and local inertial frequencies. Although some current vector records depict a slight velocity amplitude increase just above the bottom, currents are generally characterized by a rapid decrease in velocity amplitudes with increasing depth. In addition, currents at different depths are not in phase.

The probability distributions of current speeds are given in table 2 and mean current speeds are given in table 3. For many of the deep current records (below 1,000 m), current speeds are often below the threshold speed (2.5 cm/sec) of the current meters. Although the meters appear to operate satisfactorily below threshold speed, uncertainty about the meter calibration and operation below threshold speed indicates that the interpretation of the measured deeper current results should be primarily qualitative.

TIME SERIES ANALYSIS OF MEASURED CURRENTS

1. Theory

Rotary energy spectra and cross-spectra were computed using techniques described by Gonella (1972) and Mooers (1973). These techniques resolve vector current records into clockwise and anticlockwise rotating components. The east-west velocity component $U_1(t)$ and the north-south velocity component $U_2(t)$, where t is time, can be represented by their Fourier coefficients (a_1, b_1) and (a_2, b_2), respectively, as follows:

$$U_1(t) = \frac{1}{2\pi} \int_0^\infty [a_1(\sigma) \cos(\sigma t) + b_1(\sigma) \sin(\sigma t)] \, d\sigma$$

$$U_2(t) = \frac{1}{2\pi} \int_0^\infty [a_2(\sigma) \cos(\sigma t) + b_2(\sigma) \sin(\sigma t)] \, d\sigma \qquad (1)$$

The radian frequency is given by σ. The relationships between the east-west and north-south velocity components and the rotating Fourier component representation are given by:

$$U_1(t) = \frac{1}{2\pi} \int_0^\infty [A(\sigma) \cos(\sigma t + \phi(\sigma)) + C(\sigma) \cos(\sigma t + \theta(\sigma))] \, d\sigma$$

$$U_2(t) = \frac{1}{2\pi} \int_0^\infty [A(\sigma) \sin(\sigma t + \phi(\sigma)) - C(\sigma) \sin(\sigma t + \theta(\sigma))] \, d\sigma \qquad (2)$$

where A and ϕ are the amplitude and phase of the anticlockwise rotating component, and C and θ are the amplitude and phase of the clockwise rotating component. In terms of the Fourier coefficients of the east-west and north-south velocity components, the amplitudes and phases are given by:

$$A = 1/2 \left[(a_1 + b_2)^2 + (a_2 - b_1)^2 \right]^{1/2} \qquad (3)$$

$$C = 1/2 \left[(b_2 - a_1)^2 + (b_1 + a_2)^2 \right]^{1/2} \qquad (4)$$

$$\tan \phi = \frac{a_2 - b_1}{a_1 + b_2} \qquad (5)$$

$$\tan \theta = \frac{b_1 + a_2}{b_2 - a_1} \qquad (6)$$

Of particular interest for this analysis are the following rotary spectra parameters:

Clockwise energy spectrum:

$$E_C = 1/2 \, \overline{C^2} \qquad (7)$$

Anticlockwise energy spectrum:

$$E_A = 1/2 \, \overline{A^2} \qquad (8)$$

Total energy spectrum:

$$E_T = E_A + E_C = 1/2\ (\overline{A^2} + \overline{C^2}) \tag{9}$$

Rotary coefficient:

$$R_C = \frac{E_C - E_A}{E_C + E_A} \tag{10}$$

In the above and following equations, the overbar represents an average of a number of frequency contributions, that is, a band average over values determined at discrete frequencies by a finite Fourier transform.

Rotary cross-spectra were computed between selected current velocity records. For the measured currents, the dominant direction of rotation is clockwise. The coherence γ_C between clockwise rotating components is given by:

$$\gamma_C = \left[\frac{\overline{C_1 C_2 \cos(\theta_1 - \theta_2)}^2 + \overline{C_1 C_2 \sin(\theta_1 - \theta_2)}^2}{\overline{C_1^2}\ \overline{C_2^2}} \right]^{1/2} \tag{11}$$

where the subscripts 1 and 2 indicate values from different current meters. The phase difference X_C between clockwise rotating components is given by:

$$\tan X_C = \frac{-\overline{C_1 C_2 \sin(\theta_1 - \theta_2)}}{\overline{C_1 C_2 \cos(\theta_1 - \theta_2)}} \tag{12}$$

Cross-spectra between anticlockwise rotating components for different current records and between anticlockwise and clockwise components for different current records were determined using methods described by Mooers (1973).

Standard cross-spectra were also computed between selected east-west and north-south velocity components. Of primary interest is the coherence between these components. The coherence γ is given by:

$$\gamma = \left[\frac{\overline{a_1 a_2 + b_1 b_2}^{\,2} + \overline{a_1 b_2 - a_2 b_1}^{\,2}}{(\overline{a_1^2} + \overline{b_1^2})(\overline{a_2^2} + \overline{b_2^2})} \right]^{1/2} \qquad (13)$$

2. Results

Individual Fourier coefficients were determined using the complex fast Fourier transform on continuous current records equal to or longer than 28.4 days (4,096 data points). Each record was divided into sections containing 2,048 data points for both velocity components, and each section was separately transformed. No special treatment was applied to periods of very low or zero current speeds. Frequency bands were selected to place diurnal, inertial, and semidiurnal frequencies near the centers of separate frequency bands for most of the current records. To compress the analysis results at frequencies greater than 0.15 cph, a band-averaging technique was chosen to make the spectral estimates almost equally spaced when plotted versus the logarithm of the frequency. To obtain the analysis results for each current record, band averages were computed over the corresponding bands within each section of the record.

Total energy spectra are shown in figures 3 through 10. Energy spectra of currents are not shown for array A, because the record lengths are less than 28.4 days. Table 4 provides the record lengths and degrees of freedom which accompany the spectra. The 90-percent confidence bands shown on figures 3 through 10 apply to frequencies less than 0.15 cph, the region of the primary contributions to the measured currents. Each spectrum is characterized by peaks at the local inertial frequency and at the semidiurnal frequency which are indicated on the frequency scale by i and s, respectivel For arrays B, D, E, F, and G, the local inertial periods are shorter than the diurnal period, and diurnal internal wave motion cannot occur. At these arrays, the energy spectra show essentially no diurnal energy (marked by d) above a noisy background. This finding is particularly evident for the uppermost records from each location. For arrays C, H, and I, the local inertial periods are also shorter than the diurnal period but are too near the diurnal period to allow an accurate separation using the techniques which have been described.

The depth variations of energy densities for three frequency bands are shown in figure 11. The diurnal energy is within the band centered at 0.038 cph, and the semidiurnal energy is within the band centered at 0.082 cph. For arrays B, D, E, and F the inertial energy is within the band centered at 0.053 cph. For arrays C, H, and I, the inertial energy is within the band centered at 0.038 cph. The energy densities computed for array G are not included in figure 11, because spectral analysis results at only three depths may not adequately specify the energy density profile. Also presented in figure 11 is the depth variation of the Brunt-Väisälä frequency in the vicinity of the arrays. The plotted Brunt-Väisälä frequency

values were computed from STD (salinity, temperature, depth) measurements made during August 1973. The Brunt-Vaisala frequency decreases nearly exponentially with increasing depth. The kinetic energy spectrum for baroclinic internal waves is theoretically proportional to the Brunt-Vaisala frequency. The observed depth decrease of the Brunt-Vaisala frequency closely resembles the observed depth decrease of the semidiurnal energy densities. Similar comparisons have been made in the eastern North Atlantic near the Continental Shelf (e.g., Regal and Wunsch, 1973). At several locations, the semidiurnal tidal energy density increases as the bottom is approached. This may indicate that the internal tide interacts with local bottom bathymetry or that internal waves are being generated near the bottom by bottom roughness or the bottom boundary layer. Examination of the topography near the array locations showed no clear correlations between semidiurnal energy density variations near the bottom and topographic features or changes in bottom roughness. At locations where the diurnal energy is separated from the local inertial energy, the diurnal energy density is more nearly uniform with depth.

Further insight into the current structure is gained from rotary coefficients. Figure 12 provides the coefficients for current records at depths less than or equal to 1,000 m. Figure 13 provides the coefficients for current records at greater depths. The rotary coefficient is a measure of the strength of rotary motion. For currents which rotate in a perfect circle, the magnitude of the rotary coefficient is unity. The sign of the rotary coefficient is positive for clockwise rotating currents and negative for anticlockwise rotating currents. Because the current measurements were made far from continental boundaries and in the Northern Hemisphere, currents due to inertial and internal wave motion should rotate clockwise. Figures 12 and 13 show that clockwise motion is nearly always observed for frequencies at and above the local inertial frequency. At these frequencies internal waves may occur. For the records at 1,000 m which contain considerable inertial and semidiurnal energy, currents at these frequencies rotate clockwise in nearly perfect circular orbits.

For internal waves, Fofonoff (1969) has shown that the rotary coefficient is given by:

$$R_C = \frac{2\sigma f}{(\sigma^2 + f^2)} \qquad (14)$$

where f is the local Coriolis parameter. Values of R_C from equation 14 are indicated on figures 12 and 13 for latitudes bracketing all of the measurements. Below the inertial frequency, values from equation 14 are shown by a broken line to indicate that internal waves cannot occur. Observed values of the rotary coefficient compare well with equation 14 for the upper current records (fig. 12). Agreement is especially good at the local inertial and semidiurnal frequencies where energy is concentrated. Poorer agreement (fig. 13) is expected for the deeper currents,

because the low-speed currents result in a low signal-to-noise ratio and because of bottom influences.

Garrett and Munk (1972) developed an internal wave model which assumes that the internal wave field is horizontally isotropic. For isotropy, the coherence between horizontal velocity components has the same form as equation 14. That is,

$$\gamma = \frac{2\sigma f}{(\sigma^2 + f^2)} \qquad (15)$$

where γ is the coherence between the east-west and north-south velocity components. For the current records above 1,000 m, the coherences between these components are nearly identical to the rotary coefficients in figure 12.

Rotary cross-spectra were computed for simultaneous current records at the same depths less than or equal to 1,000 m at adjacent arrays and for simultaneous records at different depths on the same array. At the 1,000 m depth for arrays E and F which were 1,500 m apart, all frequency bands with significant energy (0.053 to 0.082 cph) have coherence values between clockwise rotating components greater than 0.95 and phase differences less than 31 degrees. These values for these close arrays place confidence in the measurement techniques. Except for cross-spectra between arrays E and F, no other coherence values exceed the 90-percent confidence level. Low horizontal coherences are expected because the experiment was designed with large horizontal spacings between arrays and because the most important current contributions are from inertial currents and internal waves which have horizontal scales smaller than the array spacings except for arrays E and F.

CONCLUSIONS

This description and analysis of measured intermediate and deep currents in the northeast Pacific provides the following general characteristics of the current velocity field:

1. The measured currents, particularly the mean- and low-frequency currents, have very low speeds. Low speeds are expected, because the measurements were made near the center of the eastern gyre of the North Pacific.

2. Inertial currents, which are concentrated near the surface and are incoherent over vertical distances, are a major contributor to the current structure.

3. Semidiurnal tidal frequency currents are significant. Time series analysis indicates that the oscillatory motion of semidiurnal tidal frequency is due to baroclinic internal tides rather than to barotropic surface tides. Semidiurnal tidal frequency currents are also concentrated near the surface, where the Brunt-Väisälä frequency is largest.

4. Time-dependent currents rotate clockwise.

5. Above the local inertial frequencies, the time-dependent currents are composed mainly of isotropic internal waves.

These characteristics point the way for future studies of intermediate and deep currents within the northeast Pacific. First, closely spaced arrays designed to sample small vertical and horizontal scales will be required for more detailed study of tidal frequency internal waves. Second, low current speeds may require supplementary use of Lagrangian measurement techniques such as Swallow or sofar floats. Finally, the dominant generating mechanism for the internal tides should be determined.

REFERENCES

Chhabra, N. K., Mooring mechanics, a comprehensive computer study, Charles Stark Draper Laboratory report R-775, 130 pp., 1973.

Chhabra, N. K., J. M. Dahlen and M. R. Froidevaux, Mooring dynamics experiment, determination of a verified dynamic model of the WHOI intermediate mooring, Charles Stark Draper Laboratory report R-823, 305 pp., 1974.

Fofonoff, N. P., Spectral characteristics of internal waves in the ocean, Deep-Sea Research, supplement to 16, 59-71, 1969.

Garrett, C. and W. Munk, Space-time scales of internal waves, Geophysical Fluid Dynamics, 2, 225-264, 1972.

Gonella, J., A rotary-component method for analyzing meteorological and oceanographic vector time series, Deep-Sea Research, 19, 833-846, 1972.

Guthrie, R., D. Burns and O. Smith, Current meter data report for a region of the northeastern Pacific Ocean, Tech. Note 6110-03-74, Nav. Oceanogr. Office, 1974.

Hendershott, M. C., Inertial oscillations of tidal period, in Progress in Oceanography, 6, 1-27, Pergamon Press, 1973.

Knauss, J. A., Observations of internal waves of tidal period made with neutrally buoyant floats, J. Mar. Res., 20, 111-118, 1962.

Mooers, C.N.K., A technique for the cross-spectrum analysis of pairs of complex-valued time series with emphasis on properties of polarized components and rotational invariants, Deep-Sea Research, 20, 1129-1141, 1973.

Patzert, W. C., K. Wyrtki and H. J. Santamore, Current measurements in the Central North Pacific Ocean, Rep. HIC-70-31, 65 pp., Hawaii Institute of Geophysics, 1970.

Regal, R. and C. Wunsch, M_2 tidal currents in the Western North Atlantic, Deep-Sea Research, 20, 493-502, 1973.

Reid, J. L., Jr., Observations of inertial motion and internal waves, Deep-Sea Research, 9, 283-289, 1962.

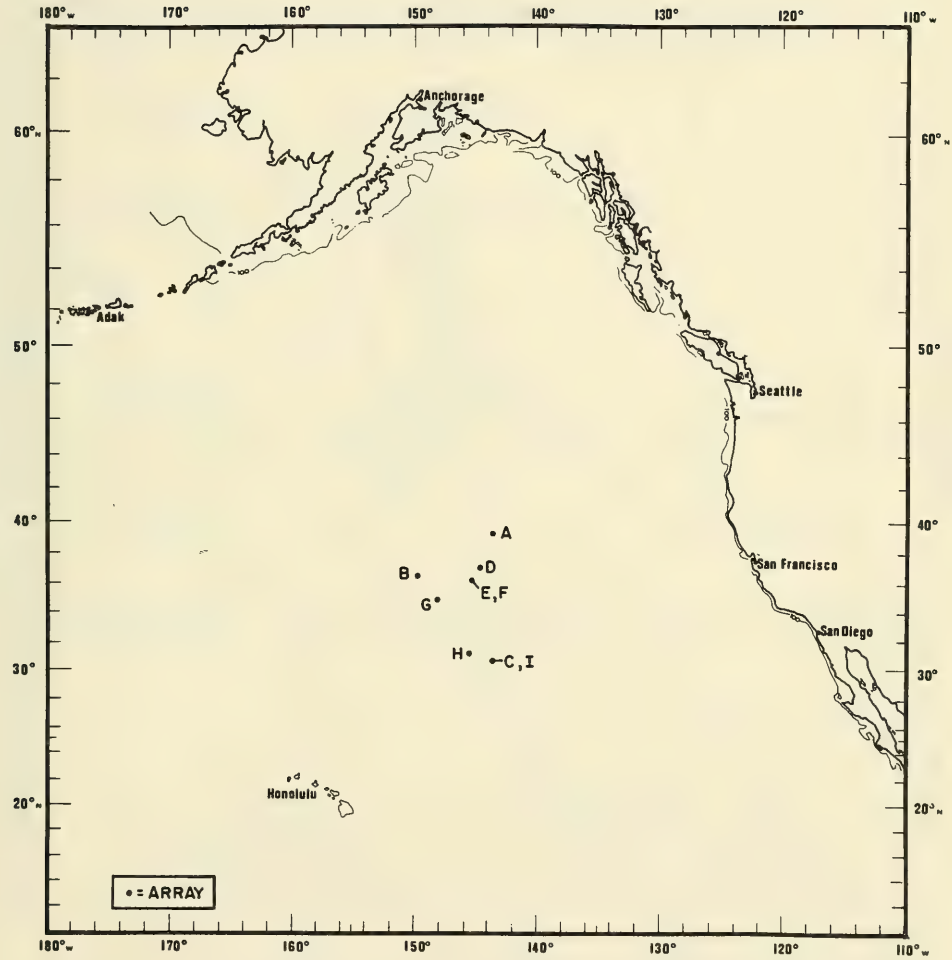

Figure 1. Locations of current measurements

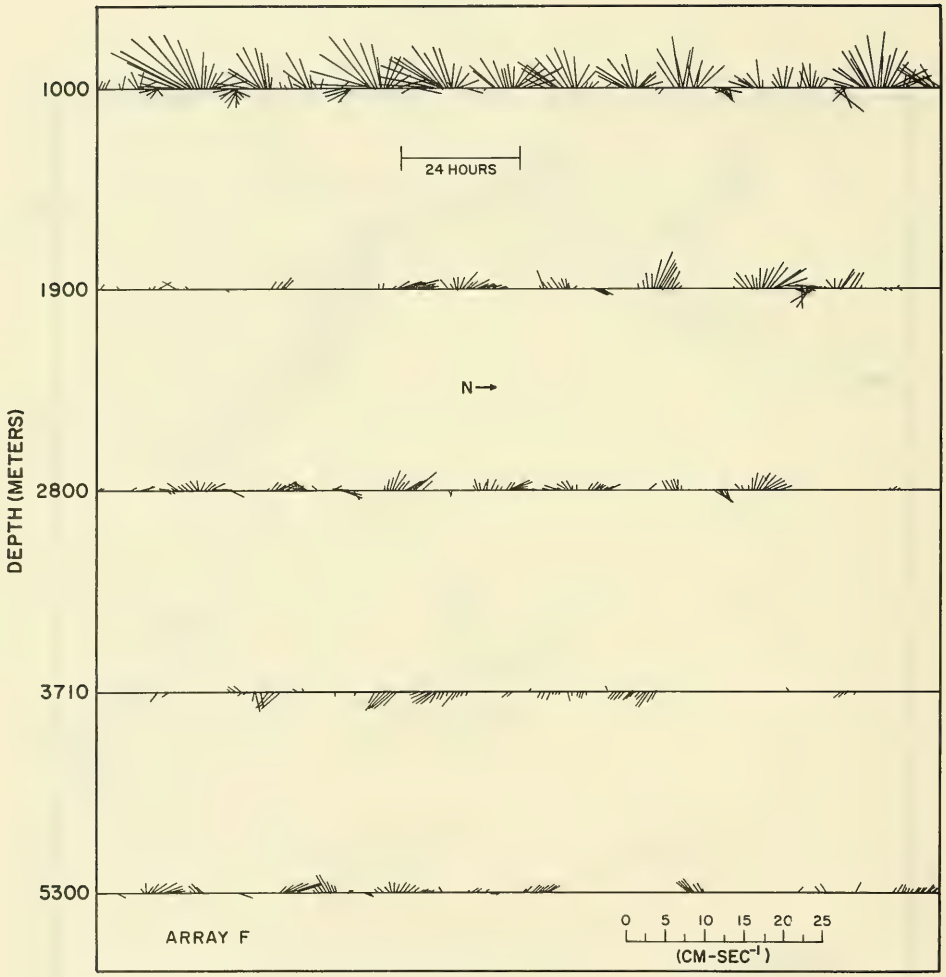

Figure 2. Example of time-dependent half-hourly current vectors

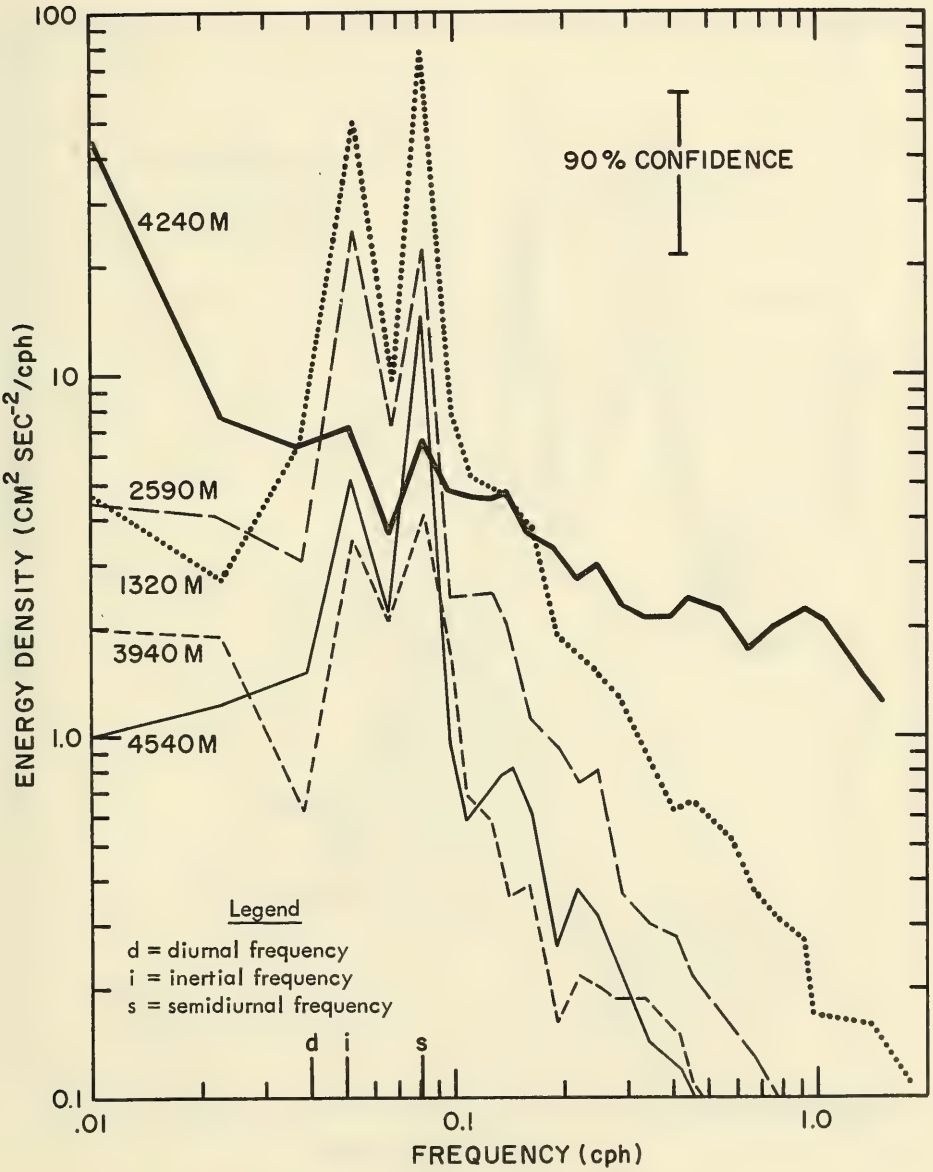

Figure 3. Energy spectra, Array B

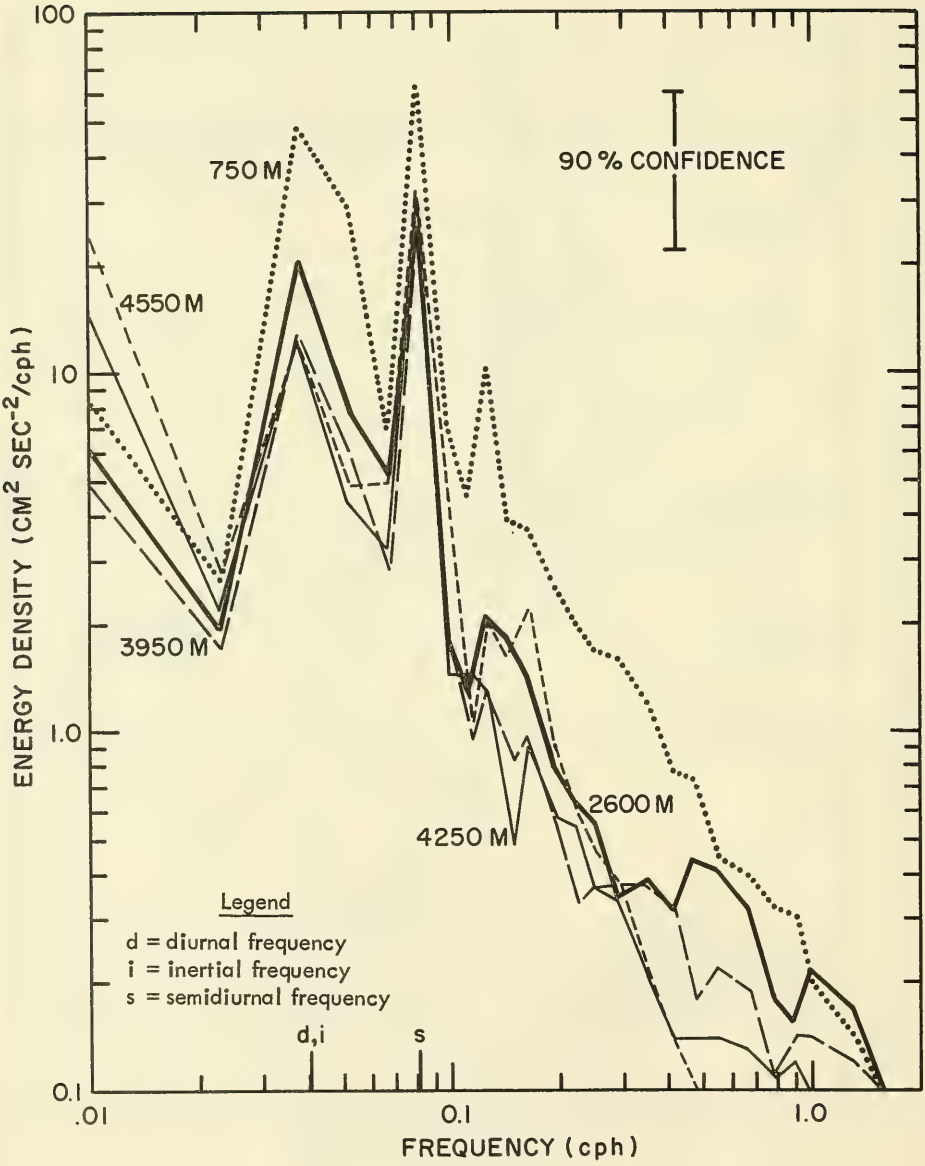

Figure 4. Energy spectra, Array C

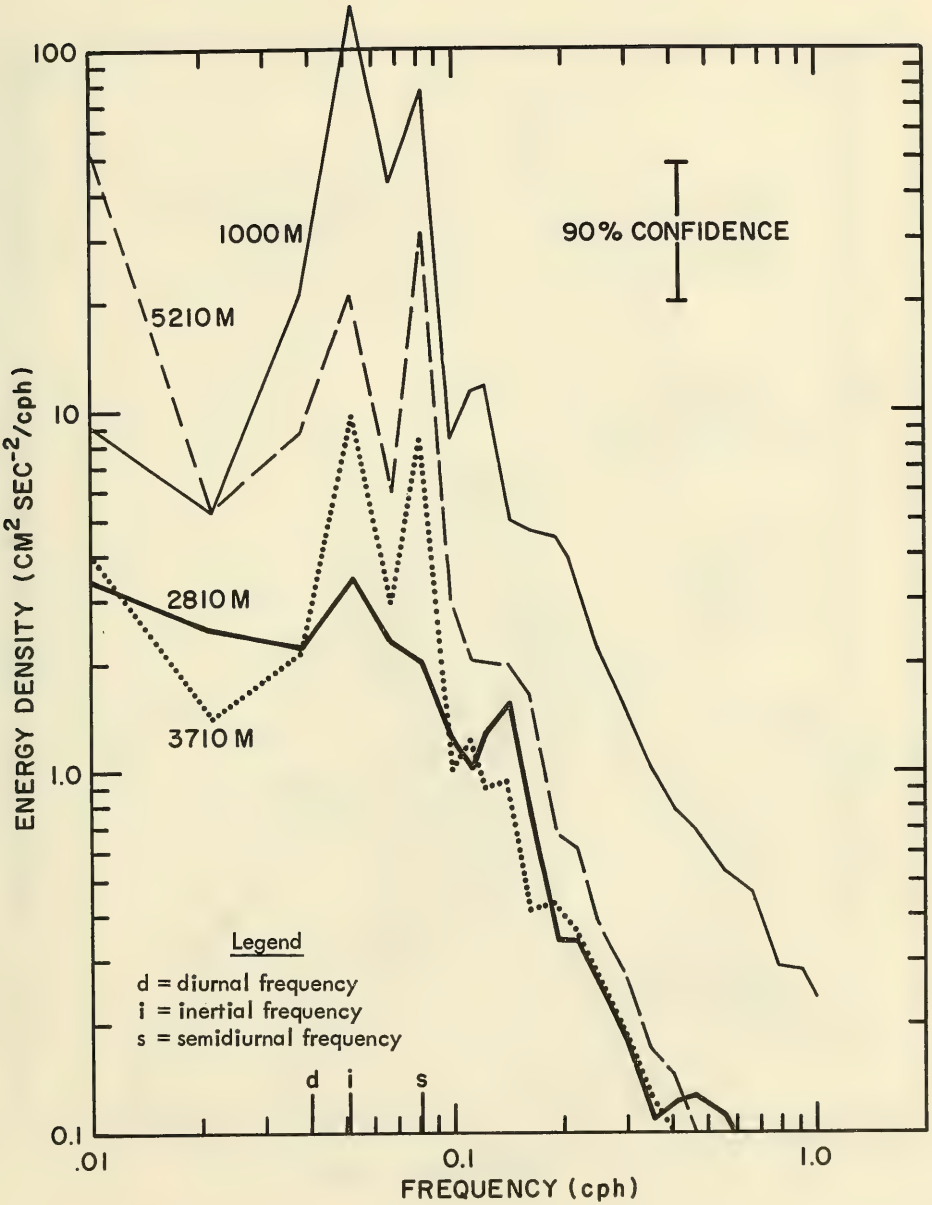

Figure 5. Energy spectra, Array D

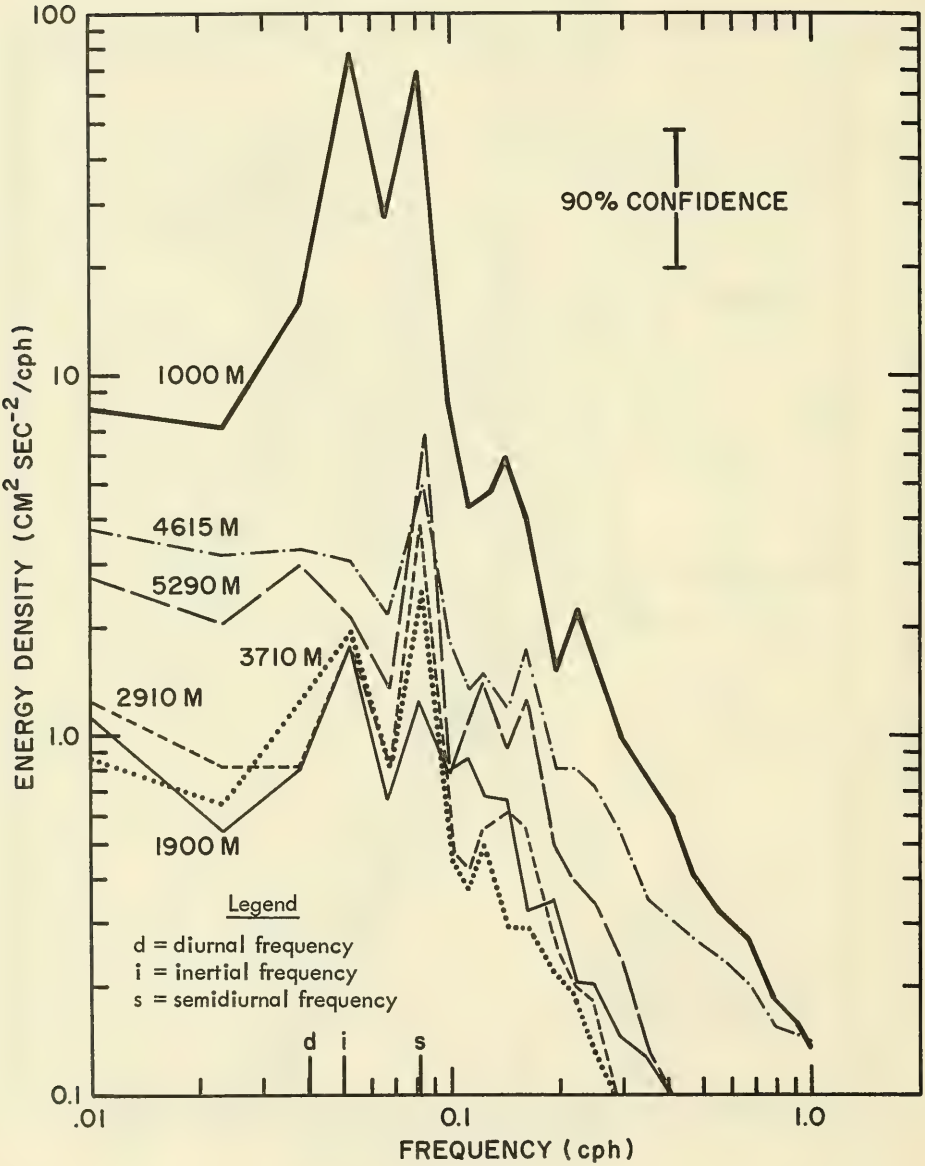

Figure 6. Energy spectra, Array E

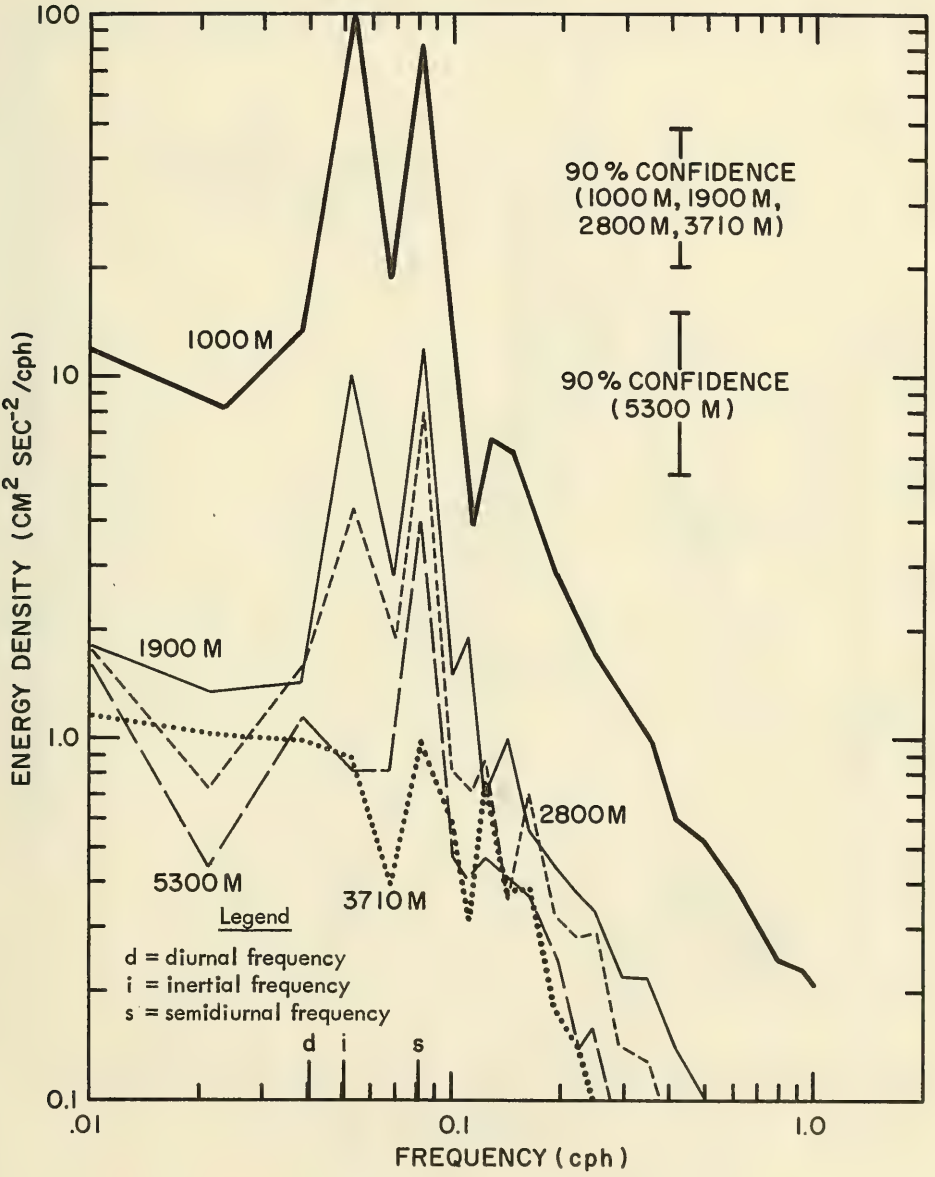

Figure 7. Energy spectra, Array F

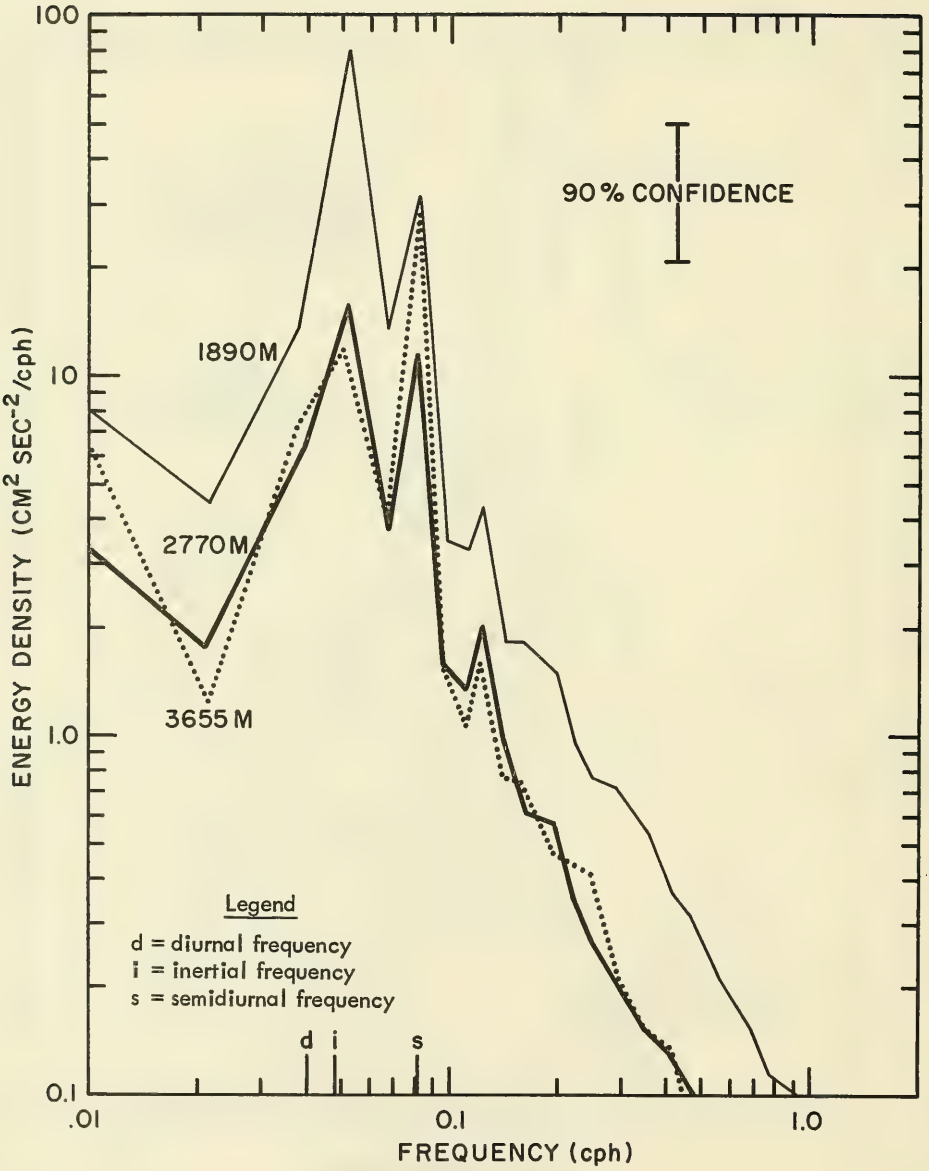

Figure 8. Energy spectra, Array G

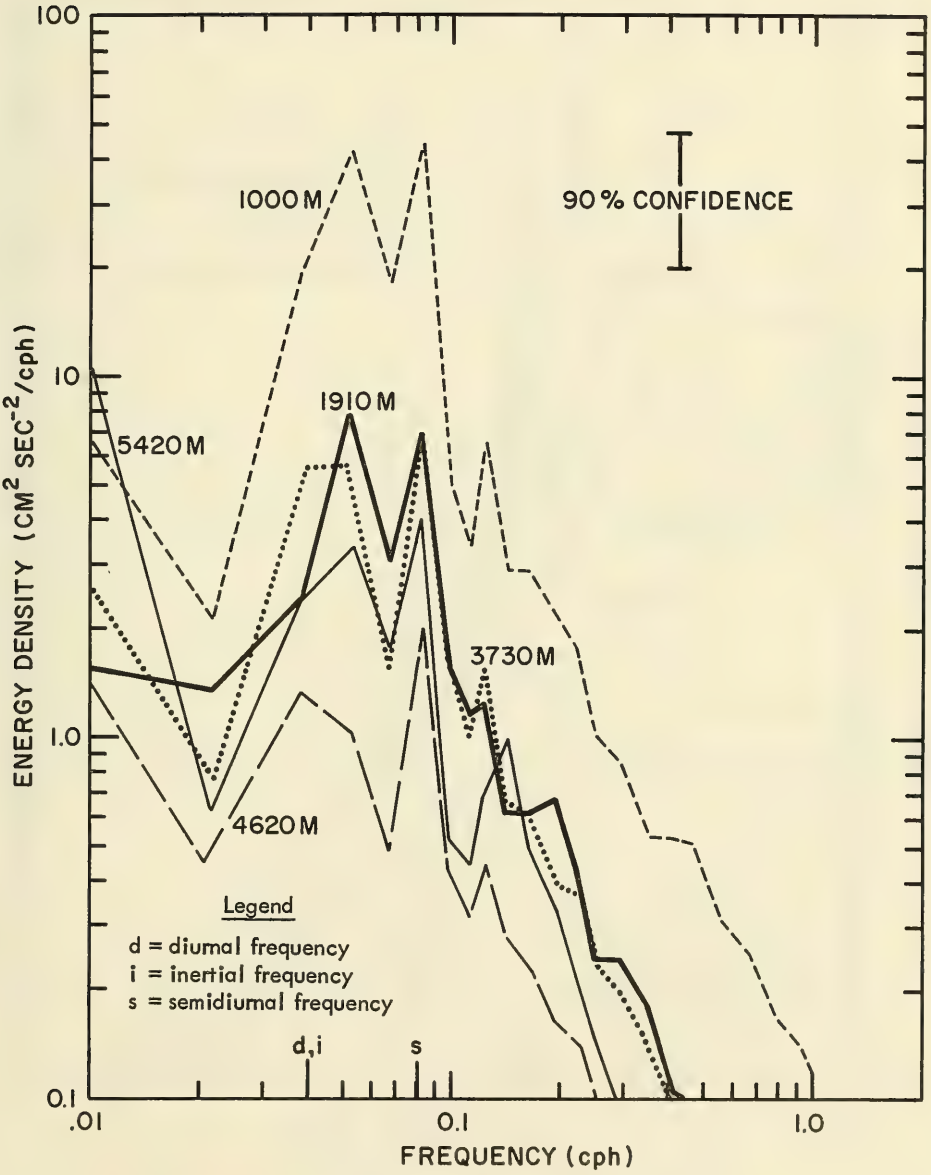

Figure 9. Energy spectra, Array H

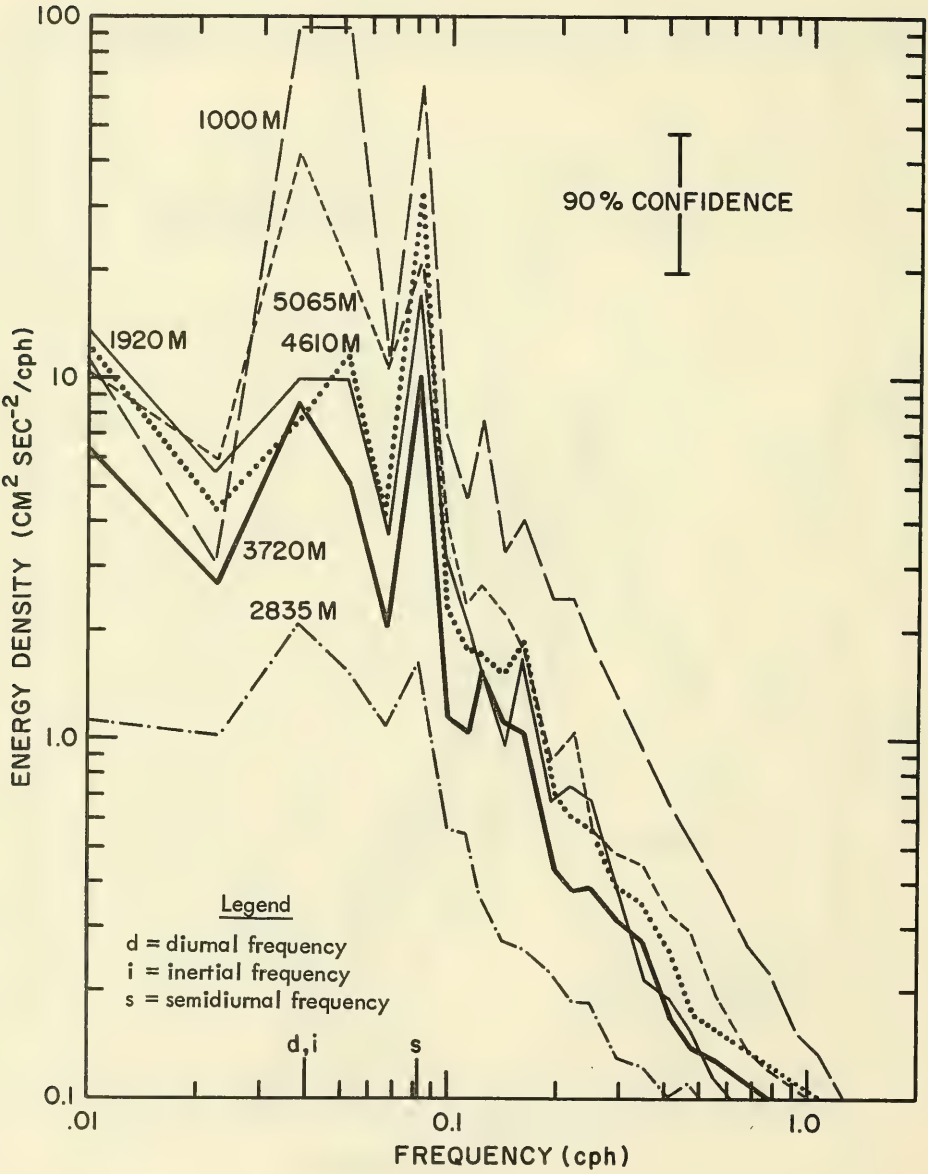

Figure 10. Energy spectra, Array I

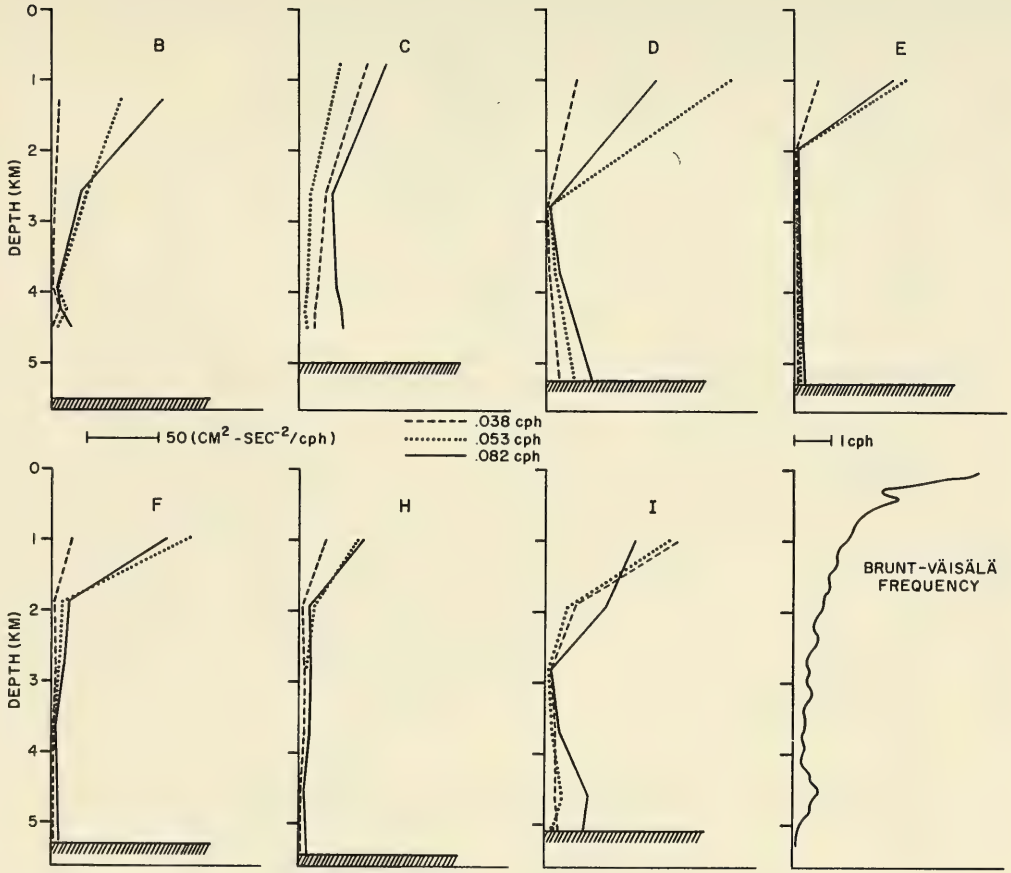

Figure 11. Depth variation of energy densities

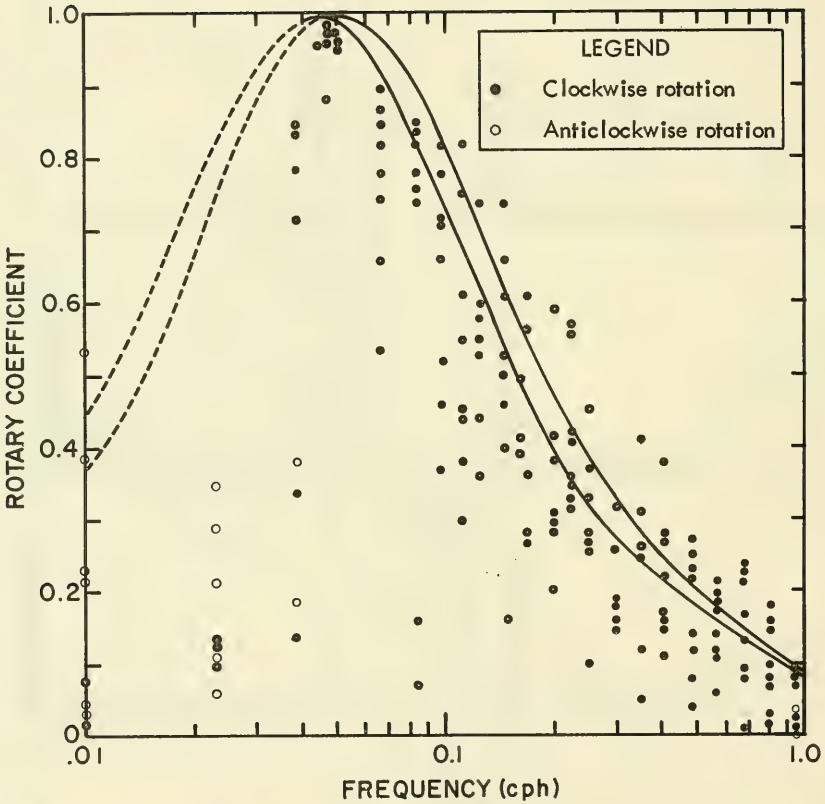

Figure 12. Rotary coefficients of current records at and above 1,000 m (The curves represent theoretical values.)

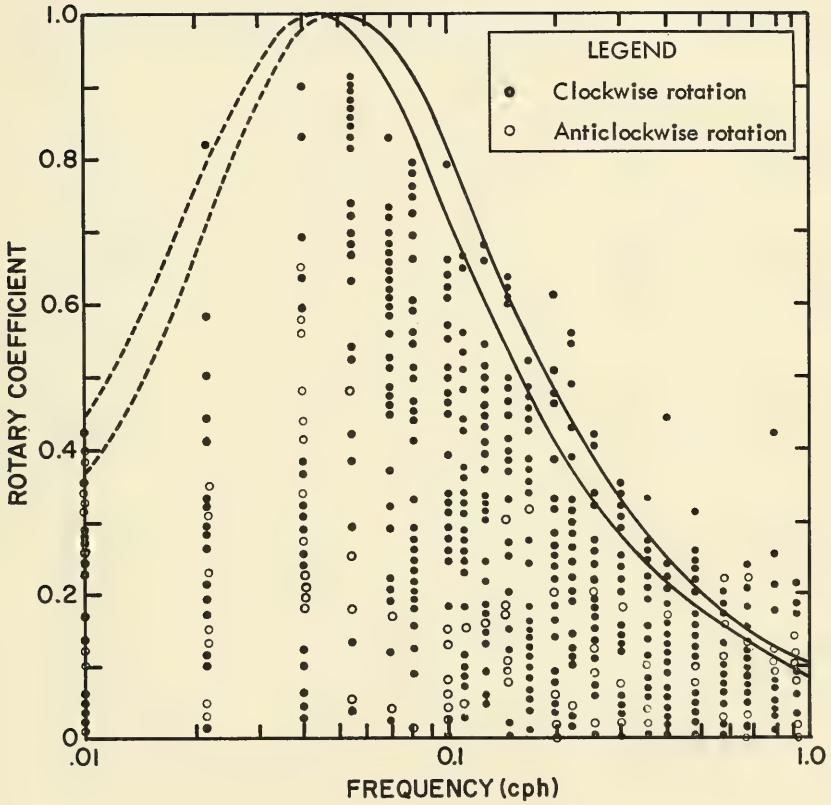

Figure 13. Rotary coefficients of current records below 1,000 m (The curves represent theoretical values.)

TABLE 1

ARRAY DESCRIPTIONS

ARRAY	METER DEPTH (M)	LAT. (N)	LONG. (E)	WATER DEPTH (M)	INERTIAL PERIOD (H)	START TIME (Z) (H, D, MO, YR)	USABLE RECORD LENGTH (D)
A	700	39°16.6'	143°35.5'	5580	18.95	1945, 30, 8, 73	26
	2500						26
	3750						26
	4050						25
	4350						26
	5525						26
B	740	36°31.0'	149°55.2'	5515	20.20	1900, 28, 8, 73	26
	1320						30
	2590						30
	3940						29
	4240						30
	4540						30
C	750	30°33.4'	143°32.3'	5025	23.60	0400, 25, 8, 73	30
	1330						Data No Good
	2600						30
	3950						30
	4250						30
	4550						30
D	1000	37°20.9'	144°52.6'	5225	19.77	1500, 20, 10, 73	56
	2810						56
	3710						56
	5210						56
E	1000	36°45.7'	145°14.5'	5300	20.03	0215, 20, 10, 73	55
	1900						55
	2910						55
	3710						55
	4615						44
	5290						52

TABLE 1 (cont.)

ARRAY DESCRIPTIONS

ARRAY	METER DEPTH (M)	LAT. (N)	LONG. (E)	WATER DEPTH (M)	INERTIAL PERIOD (H)	START TIME (Z) (H, D, MO, YR)	USABLE RECORD LENGTH (D)
F	1000	36°46.6'	145°14.3'	5315	20.03	2000, 19, 10, 73	56
	1900						56
	2800						56
	3710						56
	5300						42
G	1000	34°57.4'	148°01.3'	4380	20.94	1845, 18, 10, 73	56*
	1890						56
	2770						56
	3655						56
H	1000	31°16.4'	145°42.8'	5435	23.12	0545, 26, 10, 73	48
	1910						48
	2810						22
	3730						48
	4620						48
	5420						48
I	1000	30°35.4'	143°30.0'	5080	23.58	0530, 16, 10, 73	57
	1920						57
	2835						57
	3720						57
	4610						51
	5065						57

* CLOCK MALFUNCTION PREVENTED TIME SERIES ANALYSIS

TABLE 2

PROBABILITY DISTRIBUTIONS OF CURRENT SPEED

RECORD	SPEED CM/SEC					
	0	3	6	9	12	15
	PERCENT FREQUENCY					
A 700	71.6	24.0	4.2	0.2		
2500	95.6	2.5	1.8	0.1		
3750	95.7	2.6	1.7			
4050	93.3	3.4	1.6	0.3	1.4	
4350	98.0	2.0				
5525	92.6	6.0	1.4			
B 740	50.6	34.8	13.2	1.4		
1320	69.9	28.9	1.2			
2590	89.5	9.3	1.2			
3940	99.9	0.1				
4240	99.2	0.8				
4540	99.3	0,7				
C 750	73.5	24.1	2.4			
2600	90.8	9.2				
3950	92.4	7.4	0.2			
4250	90.6	9.4				
4550	80.3	19.5	0.2			
D 1000	65.8	27.9	6.1	0.2		
2810	97.9	2.1				
3710	96.4	3.6				
5210	51.8	27.6	17.6	3.0		
E 1000	67.8	24.5	7.3	0.4		
1900	98.9	1.1				
2910	99.4	0.6				
3710	100.0					
4615	94.4	5.2	0.4			
5290	98.6	1.4				

TABLE 2 (cont.)

PROBABILITY DISTRIBUTIONS OF CURRENT SPEED

RECORD	SPEED CM/SEC					
	0	3	6	9	12	15
	PERCENT FREQUENCY					
F 1000	61.1	28.2	9.7	1.0		
1900	97.6	2.4				
2800	99.2	0.8				
3710	99.1	0.8	0.1			
5300	98.7	1.3				
G 1000	52.9	32.2	12.1	2.5	0.3	
1890	77.9	19.8	2.3			
2770	94.0	5.8	0.2			
3655	82.4	17.4	0.2			
H 1000	77.0	21.0	2.0			
1910	97.2	2.8				
2810	98.6	1.4				
3730	97.9	2.1				
4620	99.8	0.2				
5420	96.9	3.1				
I 1000	58.3	30.7	10.3	0.7		
1920	82.9	15.7	1.4			
2835	98.6	1.3	0.1			
3720	94.0	5.9	0.1			
4610	82.5	16.4	1.1			
5065	81.3	18.2	0.5			

TABLE 3

MEAN CURRENT SPEED AND DIRECTION

RECORD	CM/SEC E-W	CM/SEC N-S	CM/SEC SPEED	DIRECTION °T
A 700	0.56	0.38	0.68	056
2500	-0.04	0.12	0.13	340
3750	-0.05	-0.01	0.05	263
4050	-0.23	-0.05	0.24	258
4350	-0.13	-0.05	0.14	249
5525	-0.08	-0.06	0.10	233
B 740	0.48	0.98	1.09	026
1320	0.59	0.57	0.82	046
2590	0.47	0.22	0.52	065
3940	0.25	-0.03	0.26	097
4240	0.50	0.18	0.53	70
4540	0.41	-0.14	0.43	109
C 750	0.78	0.02	0.78	088
2600	0.94	0.35	1.00	070
3950	0.56	0.75	0.94	037
4250	0.43	0.59	0.73	036
4550	0.64	0.98	1.12	033
D 1000	-0.45	-0.32	0.55	235
2810	0.09	-0.32	0.33	164
3710	0.31	-0.14	0.34	114
5210	2.17	-1.45	2.61	124
E 1000	-0.99	-0.44	1.08	246
1900	-0.10	-0.04	0.11	248
2910	-0.10	0.10	0.14	315
3710	-0.10	0.09	0.13	312
4615	-0.38	-0.05	0.38	262
5290	-0.23	-0.12	0.26	242
F 1000	-1.08	-0.43	1.16	248
1900	-0.14	0.03	0.14	282
2800	-0.14	0.19	0.24	324
3710	0.15	-0.14	0.21	133
5300	-0.10	0.05	0.11	297
G 1000	0.95	-2.18	2.38	156
1890	0.90	-1.17	1.48	142
2770	0.42	-0.68	0.80	148
3655	1.13	-1.50	1.88	143
H 1000	-0.26	0.10	0.28	291
1910	-0.03	0.21	0.21	352
2810	-0.02	0.13	0.13	351
3730	-0.16	0.18	0.24	318
4620	-0.08	0.05	0.09	302
5420	-0.31	0.04	0.31	277

TABLE 3 (cont.)

MEAN CURRENT SPEED AND DIRECTION

RECORD	CM/SEC E-W	CM/SEC N-S	CM/SEC SPEED	DIRECTION °T
I 1000	1.81	-0.08	1.81	092
1920	1.17	0.20	1.19	080
2835	0.17	0.06	0.18	071
3720	0.31	-0.54	0.67	120
4610	0.89	-0.94	1.33	133
5065	-1.32	-0.79	1.54	239

TABLE 4

SPECTRAL ANALYSIS PARAMETERS

Record length: 6,144 samples, 42.7 days
Degrees of freedom for frequencies $\leq$ 0.15 cph: 30
Degrees of freedom for 0.15 cph < frequencies $\leq$ 0.25 cph: 60
Degrees of freedom for 0.25 cph < frequencies $\leq$ 0.47 cph: 120
Degrees of freedom for 0.47 cph < frequencies $\leq$ 0.91 cph: 240
Degrees of freedom for frequencies > 0.91 cph: 480

Array D, all depths
Array E, all depths
Array F, 1000 m, 1900 m, 2800 m, 3710 m
Array G, 1890 m, 2770 m, 3655 m
Array H, 1000 m, 1910 m, 3730 m, 4620 m, 5420 m
Array I, all depths

Record length: 4,096 samples, 28.4 days
Degrees of freedom for frequencies $\leq$ 0.15 cph: 20
Degrees of freedom for 0.15 cph < frequencies $\leq$ 0.25 cph: 40
Degrees of freedom for 0.25 cph < frequencies $\leq$ 0.47 cph: 80
Degrees of freedom for 0.47 cph < frequencies $\leq$ 0.91 cph: 160
Degrees of freedom for frequencies > 0.91 cph: 320

Array B, 1320 m, 2590 m, 3940 m, 4240 m, 4540 m
Array C, 750 m, 2600 m, 3950 m, 4250 m, 4550 m
Array F, 5300 m

DISTRIBUTION LIST

CNO, Op-951
CNO, Op-955F
COMTHRIDFLT
CO, Canadian Maritime Forces, PAC
COMOCEANSYSPAC
COMNAVSEASYSCOM
NAVSEASYSCOM, PMS-302
COMNAVAIRSYSCOM
NAVAIRSYSCOM, AIR-540
MASWSP, ASW-11
MASWSP, ASW-111
MASWSP, ASW-13
NAVELECSYSCOM, PME-124
NAVELECSYSCOM, PME-124TA
NAVELECSYSCOM, PME-124/20
NAVELECSYSCOM, PME-124/30
NAVELECSYSCOM, PME-124/40
NAVELECSYSCOM, PME-124/60
CO, CHESDIVNAVFACENGCOM
CHESDIVNAVFACENGCOM, FPO-1E4
NAVFACENGCOM, Code PC-2 (Dr. E. Silva)
COMNAVWEASERVCOM
OCEANAV
ONR, Code 212
ONR, Code 462
ONR, Code 480
ONR, Code 483
ONR, Code 485
ONR, AESD
NUC, Code 502
NUC, Code 6540 (R. Jones)
NUSC/NLL, Code TA
NUSC/NLL, Code SA 23
DEFRESESTABPAC (Dr. Harold Grant)
Director, NRL
NRL, Code 2627
NRL, Code 8000
NRL, Code 9101
NRL, Code 8103
NRL, Code 8160
NRL, Code 8300
NAVSURWEAPCEN
FLEWEACEN, Pearl Harbor
FNWC, Monterey
NAVSHIPRANDCEN
COMNAVAIRDEVCEN
NAVAIRDEVCEN, Code 205
DDC
CIVENGRLAB (Mr. C. Nordell)
ENVPRESDSCHFAC (Dr. T. Laevastu)
CNA (Capt. C. Woods)

Arthur D. Little, Inc. (Dr. G. Raisbeck)
City University of N. Y., Dept. of Earth and Planetary Sciences (Dr. G. Neumann)
B-K Dynamics, Inc. (Mr. A. E. Fadness)
Bell Telephone Labs (Dr. T. Phillips, Mr. R. Worley)
Bolt, Beranek & Newman, Inc. (Mr. C. Burroughs)
General Electric Co., Electronic Systems Div. (Mr. H. Burkart)
Dir., Marine Physical Lab., SIO
MRP, SIO (Dr. G. B. Morris
Planning Systems, Inc. (Dr. L. P. Solomon)
RAFF Associates, Inc. (Dr. J. I. Bowen)
TRW Systems Group (Mr. R. T. Brown)
Tetra Tech., Inc. (Mr. C. Dabney)
Texas A&M Univ. (Mr. J. D. Cochrane)
Texas Instruments, Inc. (Mr. A. Kirst)
TRACOR, Inc. (Mr. J. T. Gottwald)
Underwater Systems, Inc. (Dr. M. Weinstein)
Gulf Universities Research Consortium (Mr. Ian Miller)
Lamont-Doherty Geological Observatory, Columbia Univ. (Dr. F. Malone)
Lamont-Doherty Geological Observatory, Columbia Univ. (Dr. T. Pochapsky)
WHOI (Dr. E. E. Hays)

WHOI (Dr. T. Sanford)
WHOI (Mr. R. Walden)
University of California, SIO (Dr. J. Reid, Dr. K. Kenyon)
University of Miami (Dr. S. C. Daubin)
Western Electric Co. (Mr. G. Hammond)
University of Washington, Dept. of Oceanography (Dr. B. Taft)
Massachusetts Institute of Technology, Dept. of Earth and Planetary Physics (Dr. C. Wunsch)